POWER SYSTEM STABILITY IMPROVEMENT BY TCSC CONTROLLER EMPLOYING INVASIVE WEED OPTIMIZATION (IWO) ALGORITHM APPROACH

By

Mohammad Dawood Monis (113408)
Rahmatullah (113406)
Mustapha Umar Kele (113422)

Supervised By

Ashik Ahmed
Assistant Professor
Department of Electrical and Electronic Engineering(EEE)

Islamic University of Technology (IUT)
The Organization of the Islamic Cooperation (OIC)
Gazipur-1704, Dhaka, Bangladesh
October-2012

Islamic University of Technology (IUT)
The Organization of the Islamic Cooperation (OIC)
Gazipur-1704, Dhaka, Bangladesh

Power System Stability Improvement by TCSC Controller Employing Invasive Weed Optimization (IWO) Algorithm Approach

By:

Mohammad Dawood Monis (113408)
Rahmatullah (113406)
Mustapha Umar Kele (113422)

Supervised By:

Ashik Ahmed
Assistant Professor,
Department of Electrical and Electronic Engineering(EEE)

Islamic University of Technology (IUT)
The Organization of the Islamic Cooperation (OIC)
Gazipur-1704, Dhaka, Bangladesh
October-2012

Power System Stability Improvement by TCSC Controller Employing Invasive Weed Optimization (IWO) Algorithm Approach

A Thesis Presented to
the Academic Faculty

By

Mohammad Dawood Monis	(113408)
Rahmatullah	(113406)
Mustapha Umar Kele	(113422)

In Partial Fulfillment of Requirement for the Degree of Bachelor of Science in Technical Education (BScTE) With Specialization in Instrumentation and Control Technology

Approved by
Ashik Ahmed

………………………………………
Ashik Ahmed
Project Supervisor
Dept. of Electrical & Electronic Engineering (EEE)

………………………………………
Prof. Dr. Md. Shahid Ullah
Head of the department
Electrical and Electronic Engineering (EEE)

Members:

………………………………………
Mohammad Dawood Monis (113408)

…………………………………..
Rahmatullah (113406)

………………………………………
Mustapha Umar Kele (113422)

Islamic University of Technology (IUT)
The Organization of the Islamic Cooperation (OIC)
Gazipur-1704, Dhaka, Bangladesh

October-2012

<u>Declaration</u>

This is to certify that the project entitled **"Power System Stability Improvement by TCSC Controller Employing Invasive Weed Optimization (IWO) Algorithm Approach"** is supervised by **Ashik Ahmed**. This project work has not been submitted anywhere for a degree or diploma.

………………………………………

Ashik Ahmed
Project Supervisor
Department of Electrical & Electronic Engineering (EEE)

………………………………………

Mohammad Dawood Monis (113408)
Member

……………………………………..

Rahmatullah (113406)
Member

………………………………………

Mustapha Umar Kele (113422)
Member

To our parents,

Brothers and

Sisters

Acknowledgements

First of all, we would like to express our deep and sincere gratitude to our respected supervisor **Ashik Ahmed**, assistant professor in Electrical and Electronic Engineering department of Islamic University of Technology (IUT), Dhaka, Bangladesh, for his kind guidance and supervision on this project work. His regular and well supervisions, kind helps, patience, made this project to gain its goal.

Second, we would like to express our deepest cordial thanks to our parents for their supports and tolerance of being far away from them many years. It is not really we who reached here, but of course it is our kind parents who gave us hope and inspirations.

Abstract

Due to the demands of the modern industries and households, the reliable and economic efficient utilization of electric power became a major challenge for the scientists, engineers and researchers. To fulfill those demands, it needs to interconnect large number of generators/turbines and transmit power over a very long transmission lines to the remote areas with heavy loadings, causing unstable system due to small frequency oscillations remaining and growing in the system. Traditionally Power System Stabilizers (PSS) were used to improve the power system stability. Due to reasons PSS failed, Thyristor Controlled Series Compensator (TCSC), which is a member of Flexible AC Transmission System (FACTS) family, used to improve stability instead.

In this study, the non-linear model of TCSC controller is used to improve the power system stability. The behaviors of generator parameters such as rotor angle, rotor speed, internal voltage behind X_d' and equivalent excitation voltage are tested for the deviations in the oscillation and damping response. Invasive Weed Optimization (IWO) algorithm approach is used to optimize the TCSC controller parameters for each of three different loadings. IWO algorithm searches to find out the finest suitable set of parameters for the TCSC controller parameters, the stability is much effectively improved. To prove the effectiveness of the work, the system is tested with three different loading conditions. The fast acting of the controller, in case of disturbances, is one of the major aims that this work contributed. The cost function of the IWO shows how much this algorithm is efficient for fast optimization of the parameters.

Keywords

TCSC controller, SMIB, IWO, Power System Stability

List of Figures

List of Tables

Contents

Chapter 1

INTRODUCTION

1.1 Introduction

Population growth, civilization and social developments result in industrial growth and housing electric power demand which increase the power demands day after day. So that, in order to fulfill these demands, the electrical power industries are supposed to interconnect a large number of electrical generators or turbines, feeding to long transmission lines with heavy loads. There are many factors that cause an unstable system which are mostly concerned with the dynamics of the system components such as generators, transmission lines, loads and other control equipment.

The power system stability is divided into two broad classes [1]:

1. Steady State/Small Signal Stability

   Steady state stability is a particular steady state operating condition of the system which follows any small disturbance, it reaches a steady state operating condition which is identical or close to the pre-disturbance operating condition. Steady-state stability is a function of only the operating condition. Historically steady-state instability has been associated with angle instability and slow loss of synchronism among generators.

2. Transient Stability

   A transient stable power system is the one that for a particular steady-state operating condition and for a particular (large) disturbance or sequence of disturbances if, following that (or sequence of) disturbance(s) it reaches an acceptable steady-state operating condition. Transient stability is a function of both the operating condition and the disturbance(s).

Connecting multi-machines together, using long transmission lines, heavy loading, result a large power system with proportionately weak tie-lines, causes low frequency oscillations [2]. Such oscillations may remain in the system and gradually grow up, causing severe damage to the system if not controlled by any suitable damping devices [3]. The oscillations within the plant is called local or plant mode of oscillations and the oscillations among the interconnected systems are called inter-area mode of oscillations having frequency ranges of 1.0-2.0 Hz and 0.1-1.0 Hz, respectively [4]. The lower the frequency, the more widespread are the oscillations (inter-area oscillations). An example of such small frequency oscillations in a generator rotor speed is shown in Fig.1. Traditionally, people have been using the Power System Stabilizers (PSS) for damping those oscillations and improving the power system stability, but the defect with these devices are, inappropriateness with the inter-area mode of oscillations in a large power systems and long transmission lines. Yet, many researches have been done and many damping devices are introduced. Amongst those, the power electronic development introduced the Flexible AC Transmission System (FACTS) controllers. It has been observed that the FACTS devices are able to control the system stability causing by any major disturbances such as sudden change in loads, change in transmission line parameters, fluctuation in the output of the turbine and faults etc., very quickly, improving the power system stability. Thyristor Controlled Series Compensator (TCSC) is one of the prominent members of the FACTS family, which has attracted its application market and research trends due to its reliability, efficiency and economics. It is able to schedule the power flow, decrease unsymmetrical components, reduce net loss, provide voltage support, limit short-circuit currents, mitigate the sub-synchronous resonance (SSR) phenomenon, damp the power oscillations and enhance transient stability [5]-[6]. The TCSC model consists of a capacitor bank connected in parallel with two bidirectional SCRs, which in turn is in series with a bypass inductor. In order to control the TCSC, in such a way to regulate the reactance and the degree of compensation, the SCRs firing angles must be controlled proportional [7] to the system control algorithm, which is the system parameter variation.

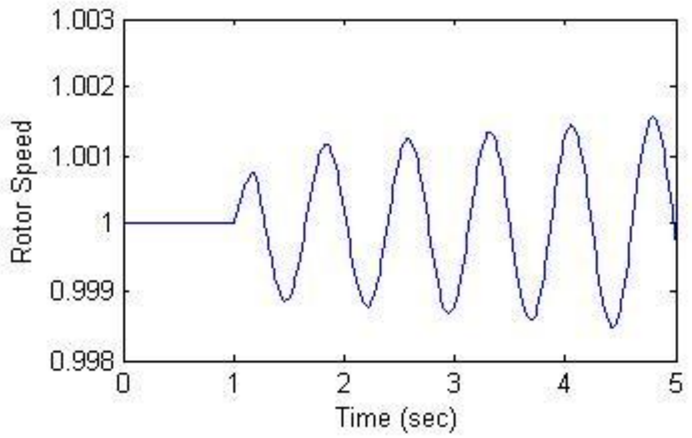

Fig.1: Rotor speed, small frequency oscillation problem

A very well-known model for synchronous generators is the Phillips-Heffron model [8]. Generally, the Single Machine Infinite Bus (SMIB) model, which consists of a generator, a transformer, a transmission line and an infinite bus, used as a sample for evaluation purposes for years that can provide a reliable and accurate result.

The optimal solution has been a big challenge yet; many techniques have been proposed to find out the optimal solution of the parameters. Recently the Invasive Weed Optimization (IWO) approach has been suggested to optimize the PSS parameters. Here, the IWO algorithm is used to optimize the TCSC controller parameters. IWO is numeric algorithm as colonized weeds, growing on a soil; finding its suitable place and position to survive in the next generation and would start reproduction. The effectiveness of IWO over other approaches is its way of production, spatial dispersal and competitive exclusion.

1.2 Method of Simulation

In this work the non-linear model of TCSC simulation for improvement of the power system stability is proposed. Invasive Weed Optimization (IWO) algorithm approach is used to optimize the system parameters of the non-linear model of TCSC. The IWO algorithm runs for several times and finally selects a set of optimal TCSC controller parameters. MATLAB is used as the simulation software.

Finally, the system is tested with three loading conditions: light loading, nominal loading and highly loading to prove the capability of the TCSC controller and the IWO optimization algorithm.

1.3 Structure of the Thesis

This thesis is divided into 4 chapters. The main objective and method of reaching to the solution of the problem is highlighted briefly in abstract part of the thesis. Thesis is aimed to start with the brief introduction to the problem and ways of reaching to the solution, modeling of the controller, introduction to the algorithm used for the optimization of the controller parameter and finally the result and conclusion regarding the work is pointed out.

Chapter 1 is dedicated to the introduction part, which declares the problem understanding, method of simulation and structure of the thesis preparation. Introduction to the Thyristor Controlled Series Compensator (TCSC), its linear and non-linear equations with initializing equations and the excitation system of the controller is discussed in chapter 2. Chapter 3 is dedicated for a brief introduction to the Invasive Weed Optimization (IWO) algorithm, used in this work. Results and conclusion of the work are illustrated and discussed in chapter 4.

Chapter 2

MODELING OF TCSC CONTROLER

A SMIB power system network which is shown in Fig.2 is under consideration in this study. The TCSC is connected in the transmission line shown in Fig.4, where X_T and X_L are the reactance of the transformer and the transmission line, respectively. V_B and V_t are the infinite bus voltage and generator terminal voltage, respectively in both figures.

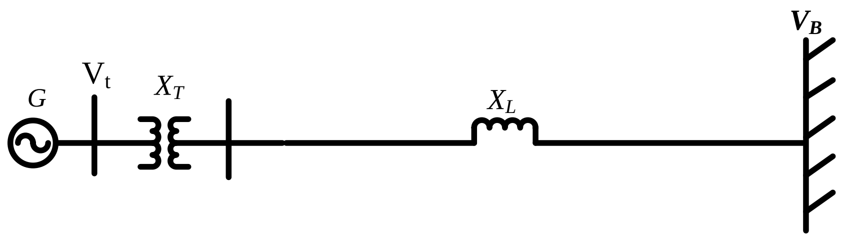

Fig.2: Single Machine Infinite Bus (SMIB) power system

2.1 Thyristor Controlled Series Compensator (TCSC)

As mentioned earlier, the TCSC is one the most important member of the FACTS family, used to improve the power system stability of the long transmission lines and the system itself in modern power systems. The effectiveness of this device is the speed of controlling active power through a transmission line which has increased its potential applications for damping of the low-frequency oscillations [9] since many years. The main circuit module for TCSC is shown in Fig.3. As shown in the figure, the TCSC module consists of a capacitor bank C, a bypass inductor L and two SCRs in bidirectional configuration SCR_1 and SCR_2. In order to control the TCSC, in such a way to regulate the reactance and the degree of compensation, the SCRs firing angles must be controlled proportional to the system control algorithm, which is the system parameter variation. In accordance to the fast switching or firing angle α or conduction angle variation characteristic of the thyristors which are controlling the TCSC, the TCSC can be a very fast device, controlling the line reactance and power system stability.

While the thyristors are being fired, it can be mathematically described by the following equations:

$$i_c = c\frac{dv}{dt} \qquad (1)$$

$$v = L\frac{di_L}{dt} \qquad (2)$$

$$i_s = i_c + i_L \qquad (3)$$

Where, i_c is the instantaneous current value in the capacitor bank and i_L is the instantaneous current value in the inductor; i_s is the instantaneous current controlled by TCSC in the transmission line and v is the instantaneous voltage across the TCSC. If we assume that the total current passes through the TCSC be sinusoidal, then the equivalent reactance of the transmission line at fundamental frequency can be X_{TCSC}. There exists a steady-state relationship between α and the reactance X_{TCSC}. This relationship can be described by the following equation, given in [2]:

$$X_{TCSC}(\alpha) = X_C - \frac{X_C^2(\sigma + \sin\sigma)}{(X_C - X_P)\pi} + \frac{4X_C^2 cos^2\left(\frac{\sigma}{2}\right)\left(\left(k\tan k\frac{\sigma}{2}\right) - \tan\frac{\sigma}{2}\right)}{\left(X_c - X_p\right)(k^2 - 1)\pi} \quad (4)$$

Where,

X_C = Nominal reactance of the fixed capacitor C.

X_p = Inductive reactance of inductor L connected in parallel with C.

$\sigma = 2(\pi - \alpha)$= Conduction angle of TCSC controller.

K= $\sqrt{\frac{x_c}{x_p}}$ = Compensation ratio

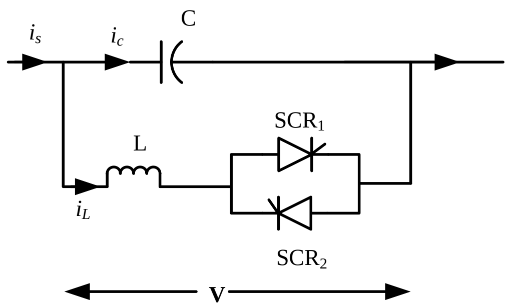

Fig.3: Configuration of a TCSC

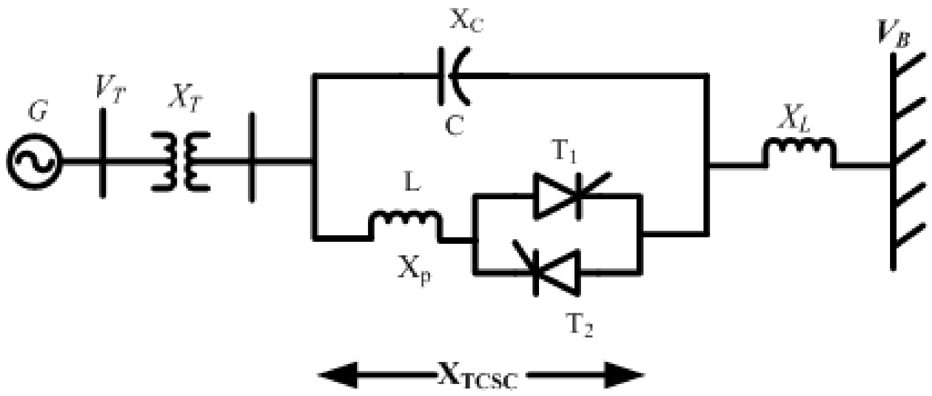

Fig.4: Single machine infinite bus power system with TCSC

2.2 The Non-linear Equations

The non-linear differential equations of the SMIB power system with TCSC used in this study are shown in a set of equation (5).

$\dot{\delta}=\omega_B(\omega-1)$
$\dot{\omega}=\frac{1}{2H}[P_m-P_e-\mathrm{D}(\omega\text{-}1)]$
$\dot{E}_q'=\frac{1}{T_{do}'}[-E_q{}'+\Delta E_{fd}-(x_d-x_d')i_d]$
$\Delta\dot{E}_{fd}=\frac{K_A}{T_A}(V_{ref}\text{-}V_t)-\frac{1}{T_A}(\Delta E_{fd})$

Where,

$P_e=v_d i_d+v_q i_q$

Let, $x_e=X_T+X_L-X_{TCSC}$

$$i_q=\frac{v_B}{x_e}\sin\delta$$

$$i_d=\frac{E_q{}'-V_B\cos\delta}{x_e}$$

$$V_t=\sqrt{v_d^2+v_q^2}$$

Where,

$v_d=x_q i_q$

$v_q=E_q{}'-x_d{}'i_d$ (5)

Where,

δ= Rotor angle

ω= Rotor speed

P_m= Mechanical input power

P_e= Electrical output power

$E_q{}'$= Internal voltage behind x_d'

E_{fd}= Equivalent excitation voltage

T_{d0}'= Time constant of excitation circuit

V_{ref}= Reference voltage

V_t= Terminal voltage

2.3 Initial Conditions

In order to solve the set of non-linear equation (5), we need the initial conditions to be defined. The following equations set of equations are used to determine the initial values.

1. $\theta_0 = sin^{-1}(\frac{P_t x_e}{V_t V_B})$
2. $\hat{I}_a = I_{a0}\angle\varphi_0 = \frac{P_t - JQ_t}{V_{t0}\angle -\theta_0}$
3. $\hat{I}_a = \frac{\hat{V}_t - E_b\angle 0}{jxe}$
4. $\hat{E}_{q0} = V_t\angle\theta_0 + jx_q I_a$
5. $E_{q0}\angle\delta_0 = V_t\angle\theta_0 + (R_a + jx_q)\ I_{a0}\angle\varphi_0$
6. $i_{d0} = I_a \sin(\delta_0 - \varphi_0)$
7. $i_{q0} = I_a \cos(\delta_0 - \varphi_0)$
8. $v_{d0} = V_{t0} \sin(\delta_0 - \theta_0)$
9. $v_{q0} = V_{t0} \cos(\delta_0 - \theta_0)$
10. $E_{fd0} = E_{q0} + (x_d - x_d')\ i_{d0}$
11. $E_{q0}' = E_{fd0} - (x_d - x_d')\ i_{d0}$
12. $E_{d0}' = (x_q - x_q')\ i_{q0}$
13. $P_e = E_{q0}' i_{q0} - E_{d0}' i_{d0} + (x_d' - x_q') i_{d0} i_{q0}$ (6)

Where, ‘0’ indicates the initial values of the system, θ is the generator terminal angle with respect to the slack (infinite) bus, i_d, i_q, v_d and v_q are the direct and quadrature armature currents and terminal voltages, respectively as shown in the diagram of Fig.5.

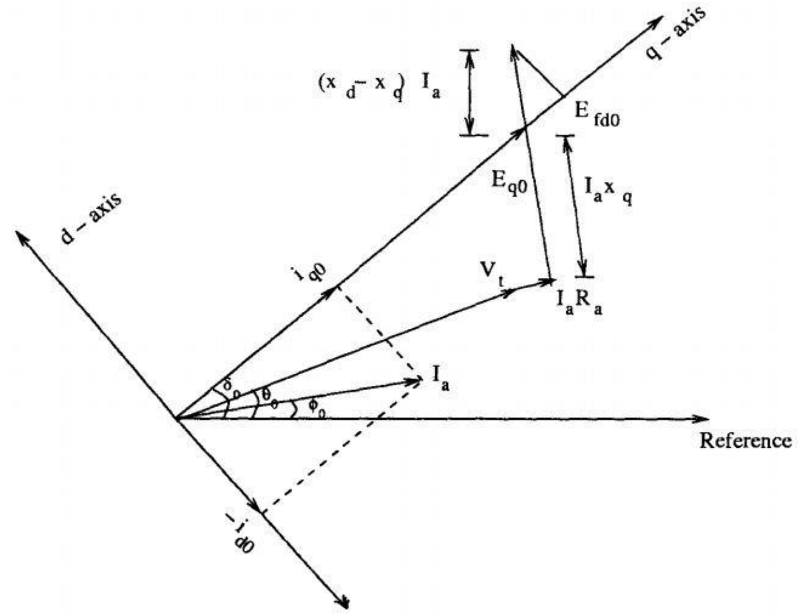

Fig.5: Phasor Diagram

2.4 Excitation System

In this study the IEEE Type-ST1A excitation system is considered, where its block diagram is shown in Fig.6. As shown in the figure, the inputs to the excitation system are V_{ref} and V_t, reference and terminal voltages, respectively. K_A and T_A are the gain and the time constant of the excitation system respectively.

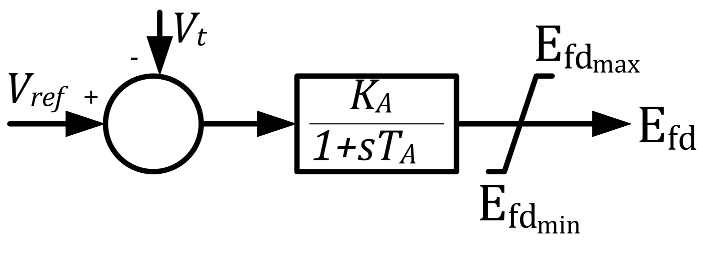

Fig.6: IEEE Type ST1A excitation system

2.5 Linearized Model

Linearizing the set of equation (5) around an operating condition of the power system, we get the following new set of equations which are also called the Phillips-Heffron model parameter of the power system with FACTS devices:

$$\Delta\dot{\delta} = \omega_b \Delta_\omega$$

$$\Delta\dot{\omega} = \left[-K_1\Delta\delta - K_2\Delta E_q{}' - K_P\Delta\sigma - D\Delta\omega\right]/2H$$

$$\Delta\dot{E}_q{}' = \left[-K_3\Delta E_q{}' - K_4\Delta\delta - K_q\Delta\sigma + \Delta E_{fd}\right]/T_{d0}{}'$$

$$\Delta\dot{E}_{fd}{}' = \left[-K_A\left(K_5\Delta\delta + K_6\Delta E_q{}' + K_V\Delta\sigma\right)\Delta E_{fd}\right]/T_A$$

Where,

$$K_1 = \frac{\partial P_e}{\partial\delta}, \qquad K_2 = \frac{\partial P_e}{\delta E_q{}'}, \qquad K_P = \frac{\partial P_e}{\partial\sigma}$$

$$K_4 = \frac{\partial E_q}{\partial\delta}, \qquad K_3 = \frac{\partial E_q}{\delta E_q{}'}, \qquad K_q = \frac{\partial E_q}{\partial\sigma}$$

$$K_5 = \frac{\partial V_t}{\partial\delta}, \qquad K_6 = \frac{\partial V_t}{\delta E_q{}'}, \qquad K_V = \frac{\delta Vt}{\delta\sigma}$$

(7)

From the set of linearized equation (7) we obtain the Phillips-Heffron model of the SMIB power system with TCSC whose block diagram is shown in Fig.7, where M= 2H.

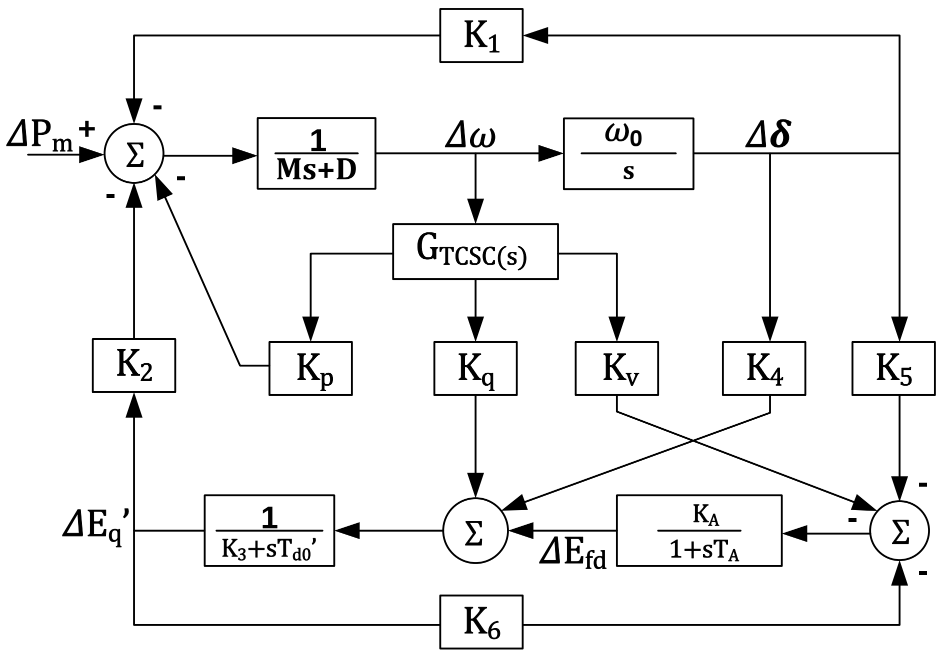

Fig.7: The Phillips-Heffron model of SMIB with G_{TCSC}

2.6 TCSC Controller Structure

In this study, a lead-lag structure which is commonly used, is considered for TCSC controller, is shown in Fig.8.

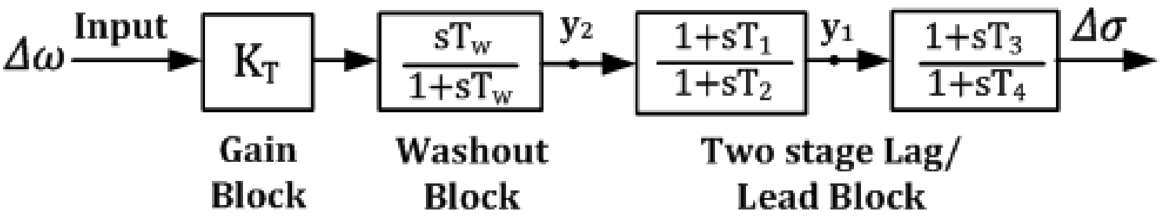

Fig.8: Structure of the TCSC controller

As shown in the Fig.8, the TCSC structure consists of a gain block K_T, a signal washout block and two stage phase compensation blocks. The signal washout block is designed such to function as a high-pass filter with its high enough time constant T_w to pass the high frequency oscillations of the input, as the same. Otherwise, with slightly changes in the input, the output would change. The time constant T_w may be assumed any value between 1 to 20 seconds. The Lag/Lead compensator blocks are so designed to compensate the phase lag/lead signals between input and output.

The derivatives of $\Delta\sigma$, y_1, y_2 which are the output of the controller and the outputs from each respective blocks, respectively, are defined by the following expressions:

$$y_2^{\cdot} = \frac{\Delta\dot{\omega} K_T T_W - y_2}{T_W} \quad (8)$$

$$y_1^{\cdot} = \frac{y_2 + \dot{y_2} T_1 - y_1}{T_2} \quad (9)$$

$$\dot{\Delta\sigma} = \frac{y_1 - \Delta\sigma + y_1 T_3}{T_4} \quad (10)$$

The K_p, K_q and K_v are the damping torques which are contributed by the TCSC. The K_p is the called the direct damping torque which is directly applied to the electromechanical oscillation loop of the generator and the K_q and K_v are called the indirect damping torque, applied through the field channel of the generator. The direct damping torque will be:

$$\Delta T_D = T_D \omega_D \Delta\omega \cong K_p K_T K_D \Delta\omega \quad (11)$$

T_D is the damping torque co-efficient.

The expression for TCSC controller is:

$$\Delta\omega = K_T\left(\frac{sT_w}{1+sT_w}\right)\left(\frac{1+sT_1}{1+sT_2}\right)\left(\frac{1+sT_3}{1+sT_4}\right)\Delta\sigma \qquad (12)$$

This is the expression obtained from Fig.8, where it is clear diagrammatically that $\Delta\omega$ is the input and $\Delta\sigma$ is the output signals of the TCSC controller. $\Delta\omega$ and $\Delta\sigma$ are the speed deviation and change in conduction angle, respectively. Here, the time constant T_w is considered to be 10 seconds. In steady state conditions the output of the controller $\Delta\sigma$ is zero and so that, $x_e = X_T + X_L - X_{TCSC}(\alpha_0)$. But, in case of dynamic conditions, the series compensation will be modulated for damping system oscillations and $x_e = X_T + X_L - X_{TCSC}(\alpha)$ and $\sigma = \sigma_0 + \Delta\sigma$, where $\sigma = 2(\pi - \alpha)$, σ_0 is the initial condition of the conduction angle and α_0 is the initial condition of the firing angle. So, the challenge is to determine optimal values for the gain K_T and time constants, T_1, T_2 , T_3 and T_4 by a suitable method, where this paper prosed the IWO Optimization approach, described in the next topic.

2.7 Objective function

We reach to a proper and effective design of TCSC controller if a proper and suitable set of values are chosen for the system parameters. The expression below describes the eigenvalue based objective function:

$$J = -min\left(\frac{real(eigenvalues)}{abs(eigenvalues)}\right) \qquad (13)$$

Maximizing the damping ratio will improve the overall damping and so that our aim is to maximize the minimum of the damping ratio for certain set of parameters. Each parameter is bounded to a certain value, and these problems can be defined as below:

Maximize J (14)
Subject to,
$K_T^{min} \leq K_T \leq K_T^{max}$ (15)
$T_1^{min} \leq T_1 \leq T_1^{max}$ (16)
$T_2^{min} \leq T_2 \leq T_2^{max}$ (17)
$T_3^{min} \leq T_3 \leq T_3^{max}$ (18)
$T_4^{min} \leq T_4 \leq T_4^{max}$ (19)

Where, J is the objective function of expression (14). As said earlier, the proposed algorithm to search for the optimized parameters is the proposed Invasive Weed Optimization (IWO) technique that will be discussed in the next chapter.

Chapter 3

INVASIVE WEED OPTIMIZATION ALGORITHM

3.1 Introduction

Previously, the IWO algorithm has been used to optimize the PSS parameters for the first time. I the effectiveness of the algorithm has been proved well. In this work, IWO is applied to optimize the TCSC controller for the first time. The Invasive Weed Optimization algorithm works the same as the weeds, colonizing on a soil, its natural behavior is simulated for the survival, position and reproduction in the next generations. The effectiveness of IWO over many other optimization approaches is its way of production, spatial dispersal and competitive exclusion.

To start the process we need to specify the initial limits of the population, where, these sets of limits would be randomly generated over the space and then the suitable member would produce seeds to distribute the population of the colony. In other words, if S_{min} be the worst member and the S_{max} be the best member, assuming that the that the seeds are randomly distributed over the space between S_{min} and S_{max} with mean equal to zero and an adaptive standard deviation (SD), where its expression for each generation is expressed below:

$$\sigma_{iter} = \frac{(iter_{max} - iter)^n}{(iter_{max})^n}\left(\sigma_{initial} - \sigma_{final}\right) + \sigma_{final} \tag{20}$$

Where,

$iter_{max}$= the maximum iteration number

σ_{iter} = the Standard Deviation (SD) at the current iteration

n = the nonlinear modulation index

The produced seeds along with their parents will be the potential solution for the next generation. The new generation will be compared and worst members would be dropped from the colonization. This process would take place until it reaches a certain optimal solutions. The flow chart, describing this process is shown in Fig.9.

3.2 The Control Parameter Selection

In equation (20) the initial and final SD, $\sigma_{initial}$, σ_{final} and n defines the characteristic of the solution. These parameters should be initialized in such a way that the best solution be obtained. Choosing high value for $\sigma_{initial}$ means to extend the search space of the algorithm and choosing smaller value for the σ_{final} means to achieve a finer optimum solution. In equation (20), the best value for n is 3. It is also stated that a value between 3 and 5 is good for the maximum number of seeds and 0 for the minimum number of seeds. The maximum excellent number of plants to be chosen for IWO is found to be between 10 and 20.

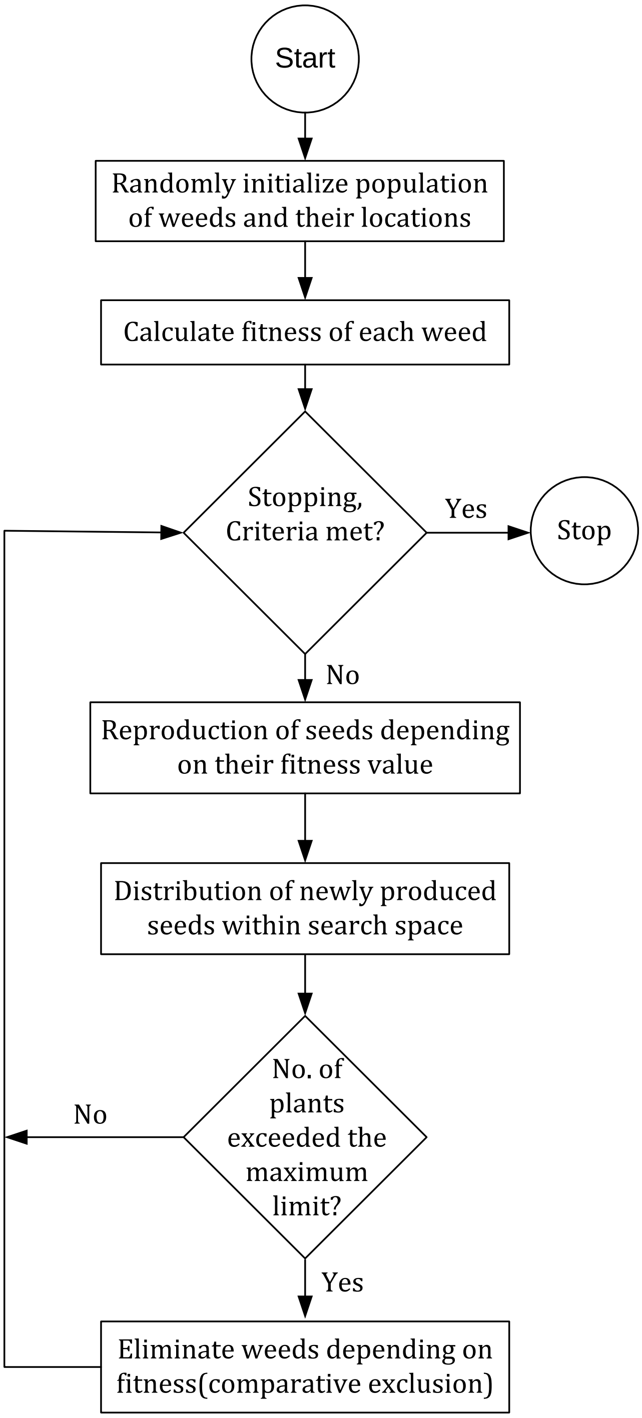

Fig.9: Flow chart of Invasive Weed Optimization algorithm

As illustrated in the flow chart of Fig.9, the algorithm starts with randomly initializing the population of weeds and their locations on space and then calculates the fitness of each seed. If the criteria for the algorithm are met, the algorithm stops search. Otherwise, depending on the fitness value, the algorithm produces seeds for the next optimization. After reproduction, the algorithm is going to spread the seeds over the search space. Due to the reproduction of seeds, the number of plants may exceed the maximum needed limit. If the number of plants exceeds the maximum limit, a comparative exclusion of the seeds according to the fitness criteria is done. Finally the criteria search is done.

Chapter 4

RESULTS

4.1 Description

The test is done on a single machine infinite bus, shown in Fig.2. The system consists of a generator, transformer, transmission line and an infinite bus. The controller is connected to the transmission line. The system is tested with three loading conditions: light loading, nominal loading and highly loading. Table 1 is showing the different loading conditions in per unit system of the different parameters.

Table 1: Loading conditions (per unit)

Conditions	Light		Nominal		Heavy	
Parameters	P_e	Q_e	P_e	Q_e	P_e	Q_e
Values	0.5	0.2	1.0	0.303	1.2	0.4

In light loading the real and reactive powers, P_e and Q_e are considered to be 0.5 and 0.2 per unit, respectively. In nominal loading the real and reactive powers, P_e and Q_e are considered 1.0 and 0.303 per unit, respectively, whereas in heavy loading, the real and reactive powers, P_e and Q_e are considered 1.2 and 0.4 per unit, respectively. Each loading are tested with and without TCSC controller.

4.2 Eigenvalue Analysis

As mentioned earlier, three loading conditions are considered to prove the effectiveness of the TCSC controller where IWO optimization algorithm is used to find out the best suitable parameters of the TCSC controller. The IWO algorithm runs several times and finally optimal sets of finest parameters will be selected. The eigenvalue analysis for selecting the optimal parameter convergences for each case is shown in Fig.10, Fig.11 and Fig.12. The figures show that how fast the IWO algorithm reaches to the finest parameters. The system damping ratios and eigenvalues with and without TCSC controller for three different loading conditions are shown in Table 3 and 4, respectively.

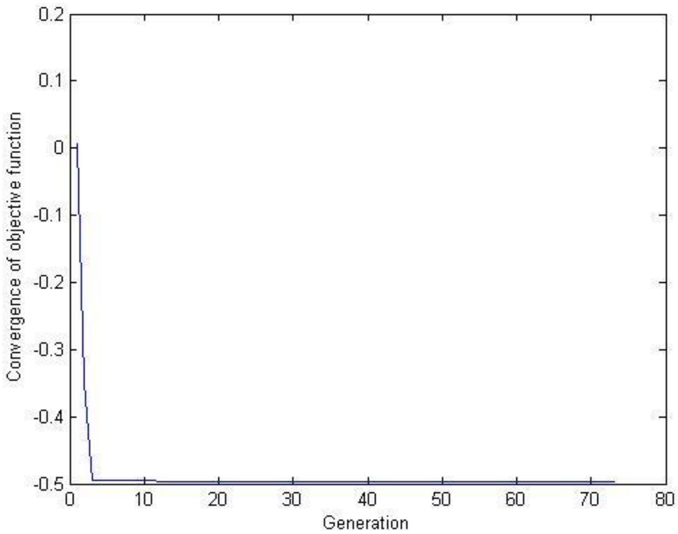

Fig.10: Cost function convergence of the parameters for light loading

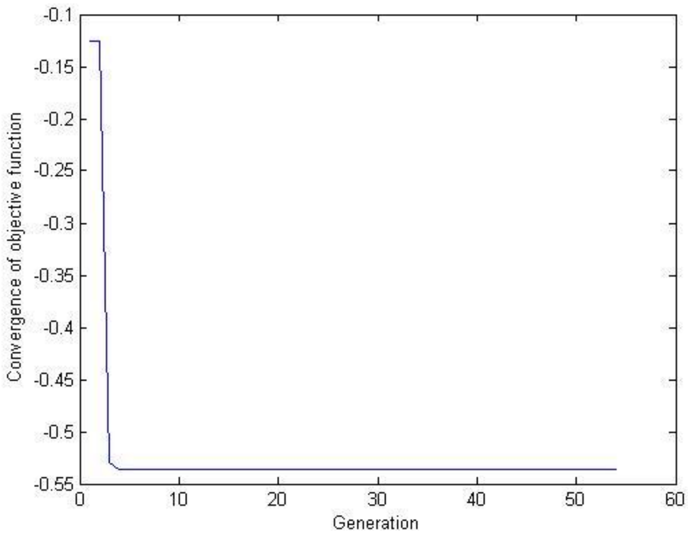

Fig.11: Cost function convergence of the parameters for nominal loading

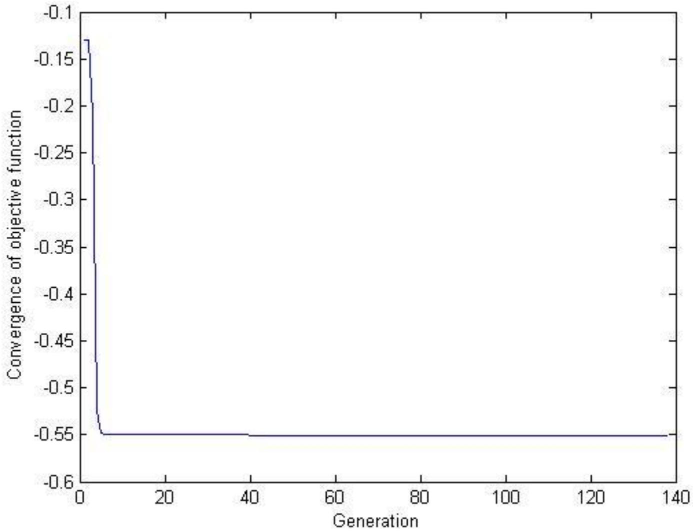

Fig.12: Cost function convergence of the parameters for heavy loading

4.3 TCSC Controller Parameter Results

In order to show the effectiveness of the TCSC controller to improve the power system stability, the simulation is done on a single machine infinite bus shown in Fig.2. The system is checked with and without TCSC on three loading conditions to prove the capability of the TCSC controller. The optimized parameters of the controller by IWO algorithm on three different loading conditions are shown in Table 2.

Table 2: Set of optimized TCSC controller parameters obtained by IWO algorithm

Parameters	Light	Nominal	Heavy
K_T	166.5661	232.4586	500
T_1	1.0	0.9029	0.5829
T_2	0.8768	0.6923	1.0
T_3	0.8898	0.6859	0.7971
T_4	0.3873	0.8115	1.0

Table 3: System eigenvalues without TCSC controller for three conditions

Light	Nominal	Heavy
-12.781 + 21.635i	-13.1905 + 20.390i	-13.453 + 19.914i
-12.781- 21.635i	-13.190 - 20.389i	-13.453 - 19.914i
0.101 + 8.500i	0.510 + 9.056i	0.773 + 9.175i
0.101 - 8.500i	0.510 - 9.100i	0.773 - 9.175i

Table 4: System eigenvalues with TCSC controller for three conditions

Light	Nominal	Heavy
-12.232 + 21.393i	-12.581 + 19.831i	-12.530 + 18.940i
-12.232 - 21.393i	-12.581 - 19.831i	-12.530 - 18.940i
-4.542 + 7.925i	-5.373 + 8.453i	-6.101 + 9.194i
-4.542 - 7.925i	-5.373 - 8.453i	-6.101 - 9.194i
-1.141 + 0.000i	-1.444 + 0.000i	-1.026 + 0.000i
-0.090 + 0.000i	-0.088 + 0.000i	-0.076 + 0.000i
-1.063e-14 + 0i	-1.742e-13 + 0.0i	-2.724e-14 + 0i

4.4 Without TCSC Parameter Responses

The effect of oscillation problem over the system parameters need to be illustrated in order to show the effectiveness of the TCSC controller. So that, the effect of small frequency oscillations on the system parameters that we deal with, such as rotor angle (δ), rotor speed (ω), internal voltage behind X_d' ($E_q{}'$) and equivalent excitation voltage (ΔE_{fd}) due to oscillations, without TCSC controller, with three different conditions are shown below.

4.4.1 Light Loading

In light loading, per unit values for real and reactive powers are considered to be 0.2 and 0.5, respectively. The responses of the rotor angle ($\boldsymbol{\delta}$), rotor speed ($\boldsymbol{\omega}$), internal voltage behind X_d' ($\boldsymbol{E_q{}'}$) and equivalent excitation voltage ($\Delta \boldsymbol{E_{fd}}$) are illustrated in Fig. 13, 14, 15 and 16, respectively.

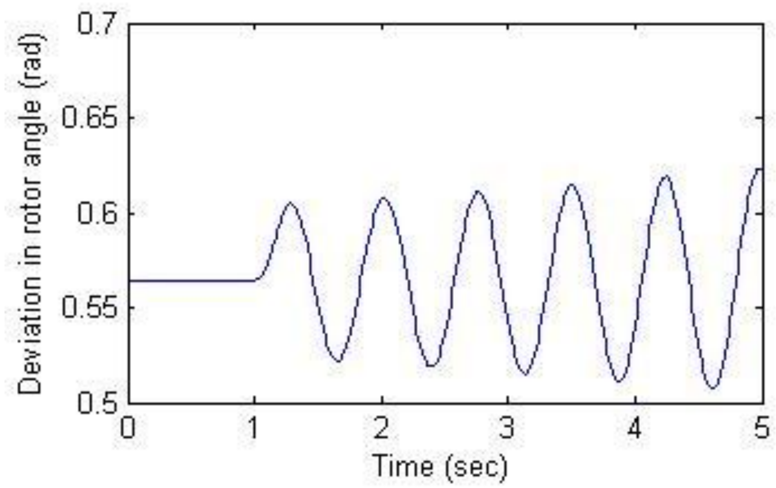

Fig.13**:** Response of Rotor angle (δ)

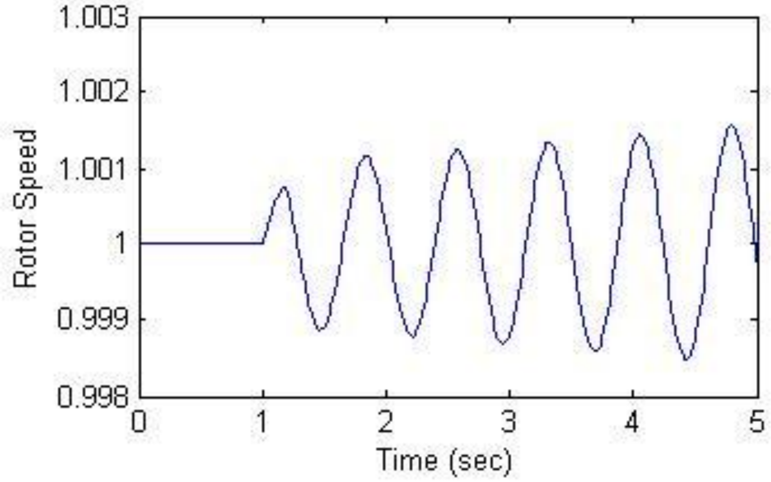

Fig.14**:** Response of Rotor Speed (ω)

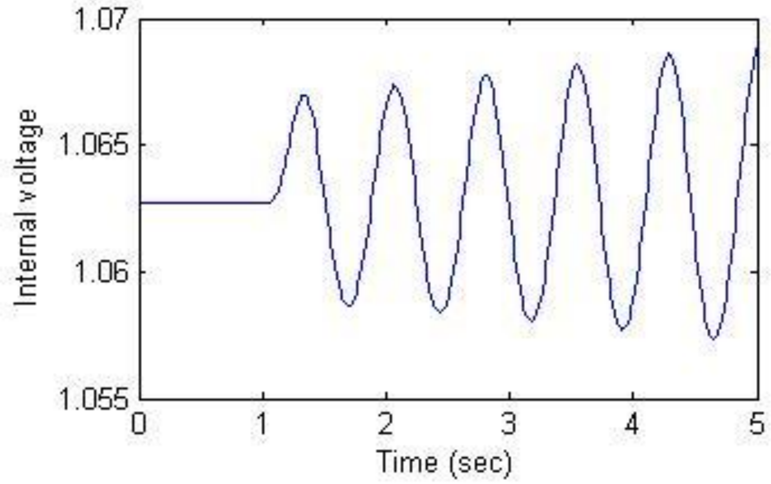

Fig.15**:** Response of Internal voltage behind X_d' ($E_q{}'$)

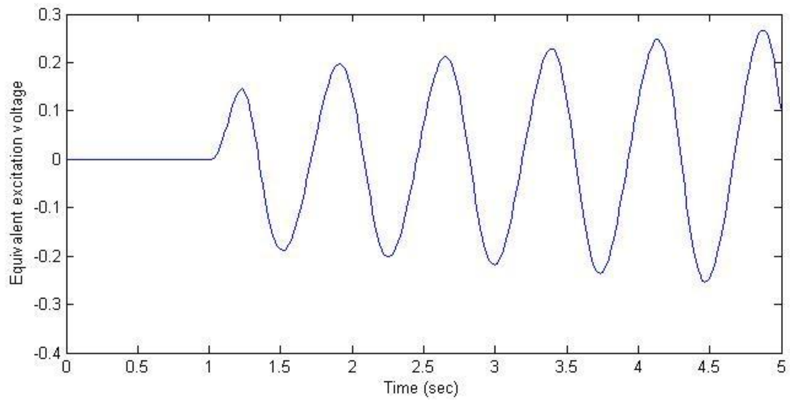

Fig.16**:** Response of Equivalent Excitation Voltage (ΔE_{fd})

4.4.2 Nominal Loading

In nominal loading, per unit values for real and reactive powers are considered to be 1.0 and 0.303, respectively. The responses of the rotor angle ($\boldsymbol{\delta}$), rotor speed ($\boldsymbol{\omega}$), internal voltage behind X_d' ($\boldsymbol{E_q}'$) and equivalent excitation voltage ($\Delta\boldsymbol{E_{fd}}$) are illustrated in Fig. 17, 18, 19 and 20, respectively.

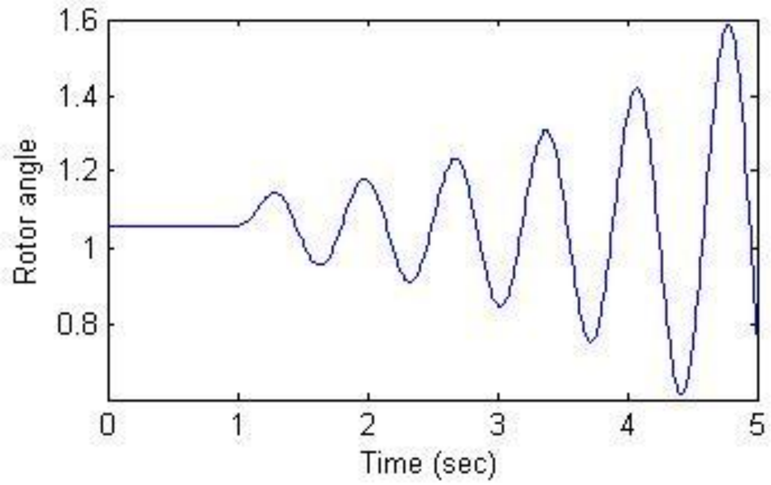

Fig.17**:** Response of Rotor angle (δ)

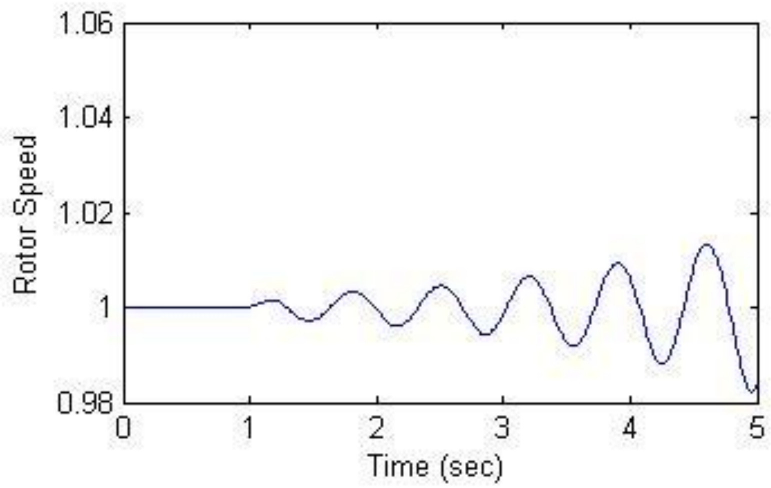

Fig.18**:** Response of Rotor Speed (ω)

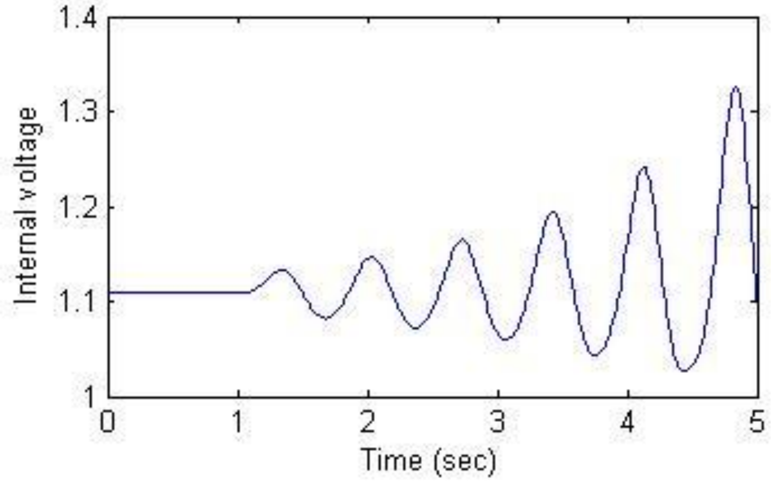

Fig.19**:** Response of Internal voltage behind X_d' ($E_q{}'$)

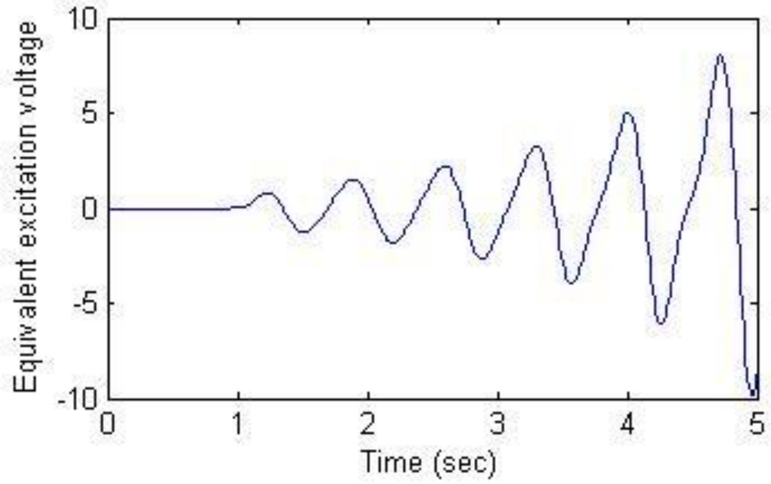

Fig.20**:** Response of Equivalent Excitation Voltage (ΔE_{fd})

4.4.3 Heavy Loading

In heavy loading, per unit values for real and reactive powers are considered to be 1.2 and 0.4, respectively. The responses of the rotor angle ($\boldsymbol{\delta}$), rotor speed ($\boldsymbol{\omega}$), internal voltage behind X_d' ($\boldsymbol{E_q}'$) and equivalent excitation voltage ($\Delta \boldsymbol{E_{fd}}$) are illustrated in Fig. 21, 22, 23 and 24, respectively.

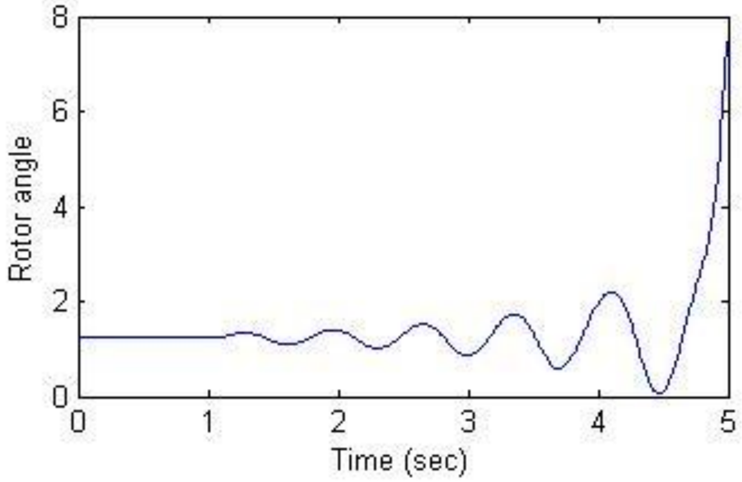

Fig.21**:** Response of Rotor angle (δ)

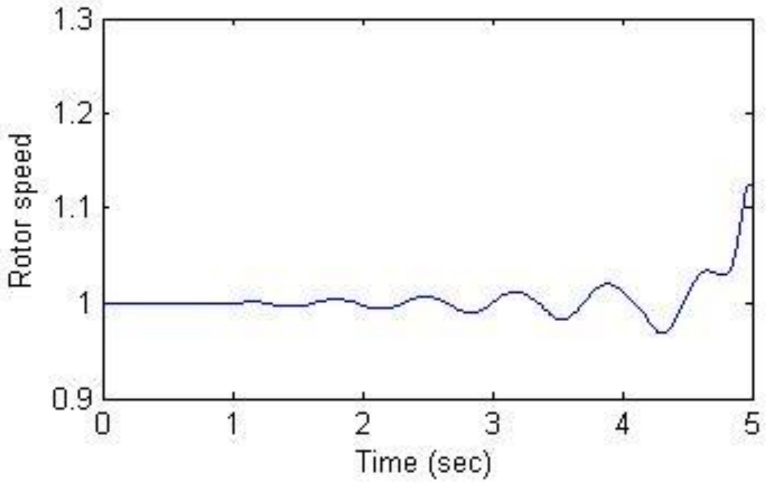

Fig.22**:** Response of Rotor Speed (ω)

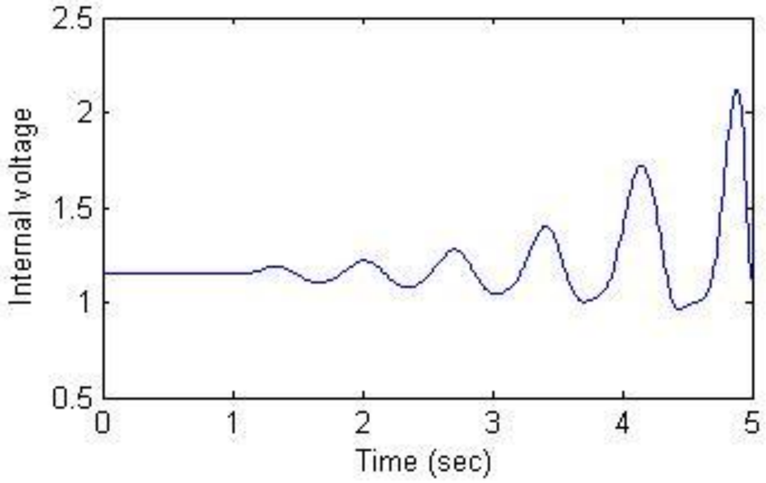

Fig.23**:** Response of Internal voltage behind X_d' ($E_q{}'$)

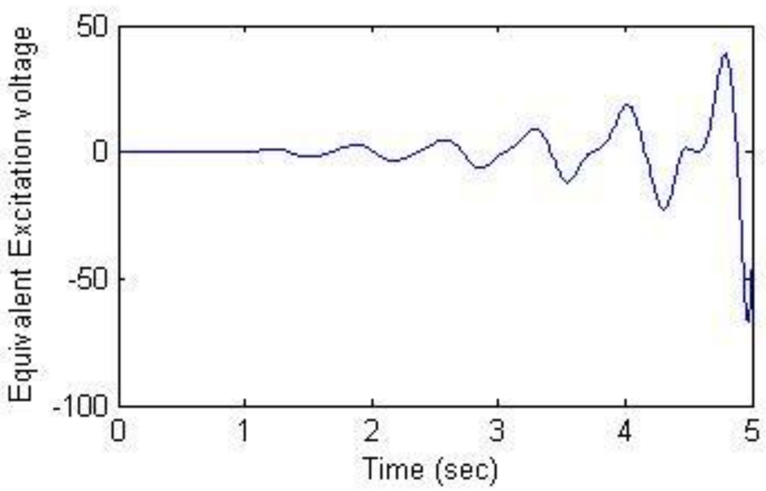

Fig.24**:** Response of Equivalent Excitation Voltage (ΔE_{fd})

4.5 With TCSC Parameter Responses

The response of different parameters due to oscillation problems were illustrated in the previous section. Now, we check the effectiveness of the TCSC controller for damping of the oscillations. The effect of the TCSC controller over the system parameters in three different loadings are illustration below.

4.5.1 Light Loading

As mentioned earlier, in light loading, per unit values for real and reactive powers are considered to be 0.2 and 0.5, respectively. The TCSC controller signal is shown in Fig.25. It is to be mentioned that the controller signal is common for all the cases, but it is put in every cases may be due to the need of clear and easy comparison of the controller signal with the oscillation problem signals. The responses of the rotor angle ($\boldsymbol{\delta}$), rotor speed ($\boldsymbol{\omega}$), internal voltage behind X_d' ($\boldsymbol{E_q}'$) and equivalent excitation voltage ($\Delta \boldsymbol{E_{fd}}$) are illustrated in Fig. 26, 27, 28 and 29, respectively.

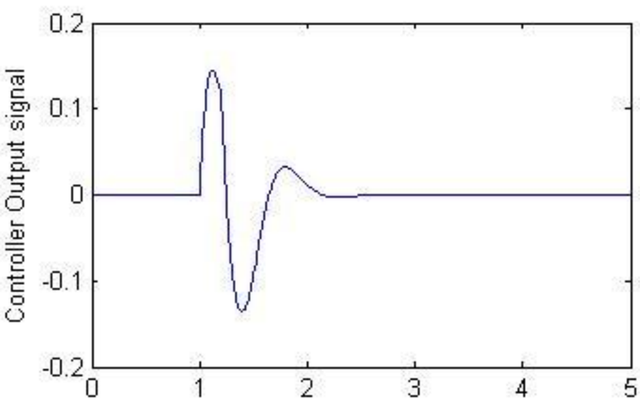

Fig.25: Response of the controller output ($\Delta\sigma$)

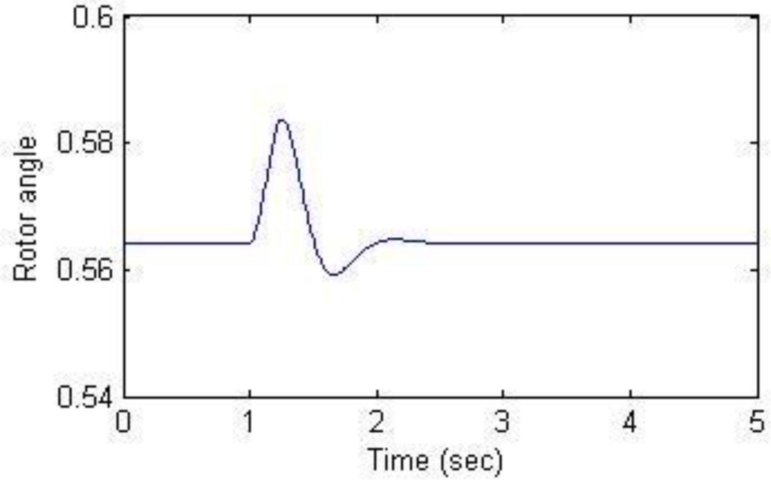

Fig.26: Response of Rotor angle (δ)

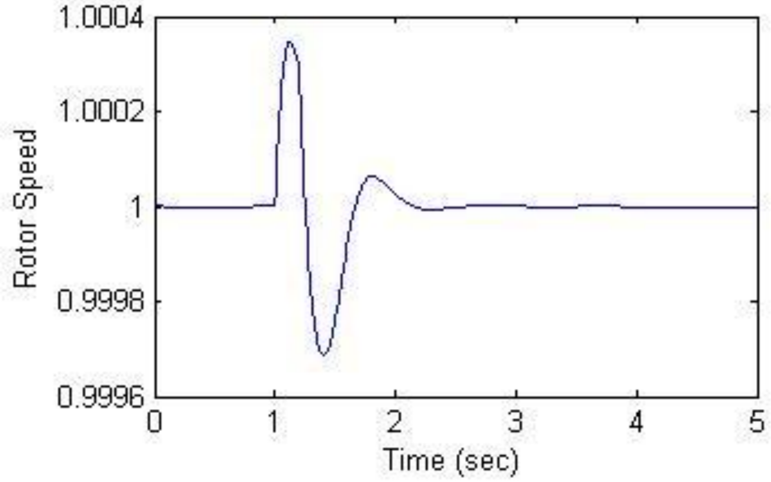

Fig.27: Response of Rotor Speed (ω)

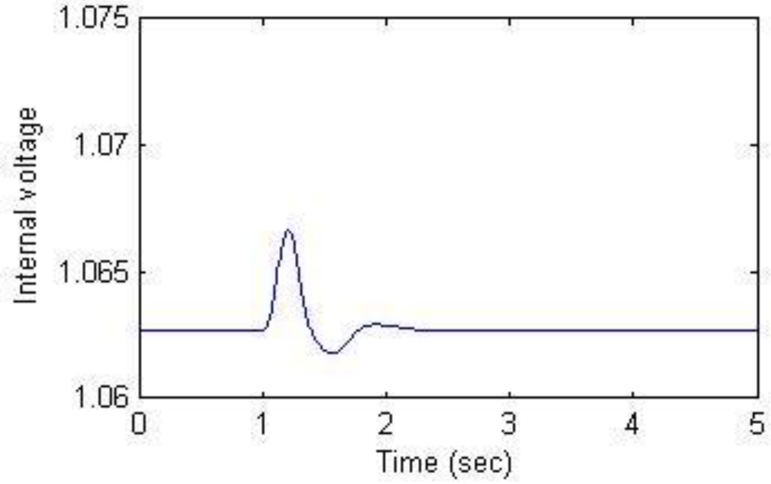

Fig.28: Response of Internal voltage behind X_d' ($E_q{}'$)

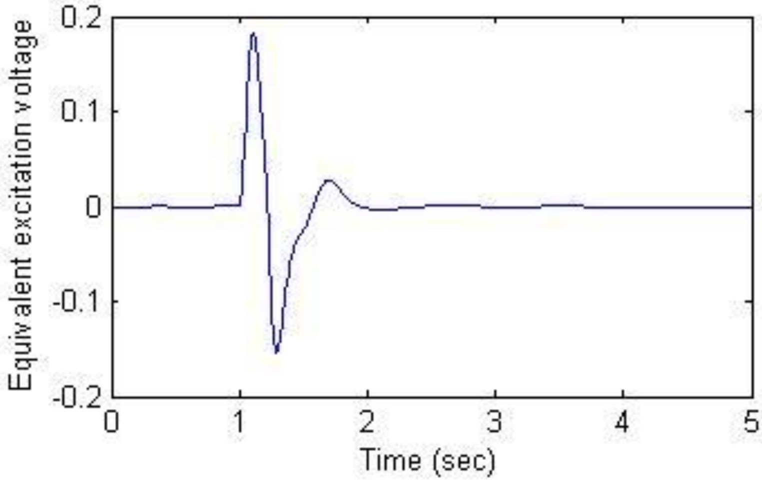

Fig.29: Response of Equivalent Excitation Voltage (ΔE_{fd})

4.5.2 Nominal Loading

As mentioned earlier, in case of nominal loading, per unit values for real and reactive powers are considered to be 1.0 and 0.303, respectively. The TCSC controller signal is shown in Fig.30. It is to be mentioned that the controller signal is common for all the cases, but it is put in every cases may be due to the need of clear and easy comparison of the controller signal with the oscillation problem signals. The responses of the rotor angle ($\boldsymbol{\delta}$), rotor speed ($\boldsymbol{\omega}$), internal voltage behind X_d' ($\boldsymbol{E_q}'$) and equivalent excitation voltage ($\Delta \boldsymbol{E_{fd}}$) are illustrated in Fig.31, 32, 33 and 34, respectively.

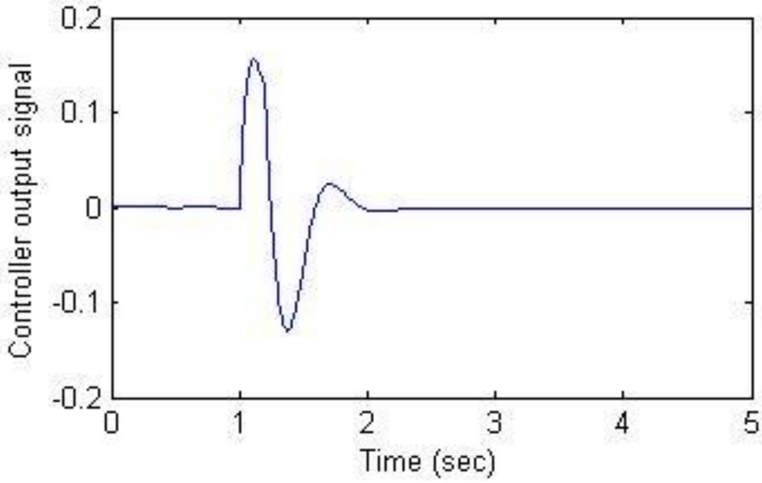

Fig.30: Response of the controller output ($\Delta\sigma$)

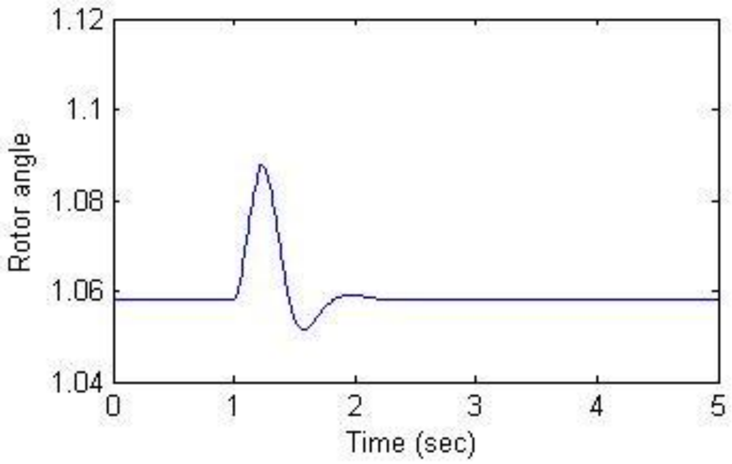

Fig.31: Response of Rotor angle (δ)

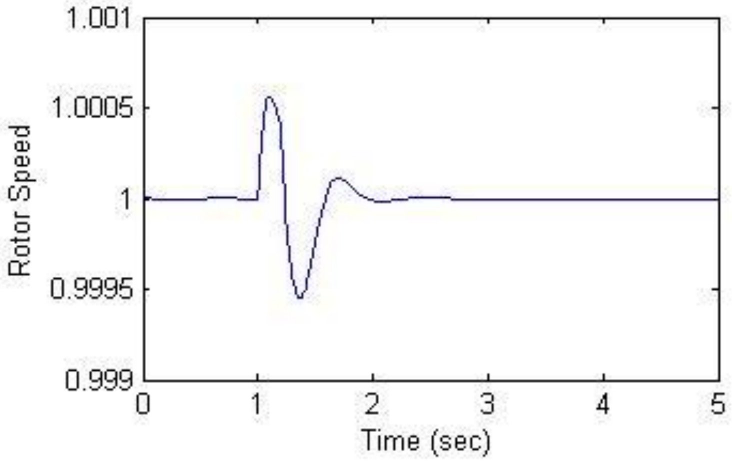

Fig.32: Response of Rotor speed (ω)

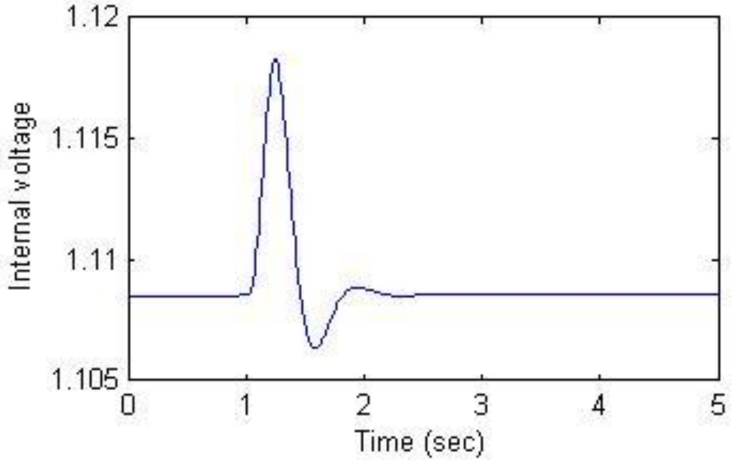

Fig.33: Response of Internal voltage behind X_d' ($E_q{}'$)

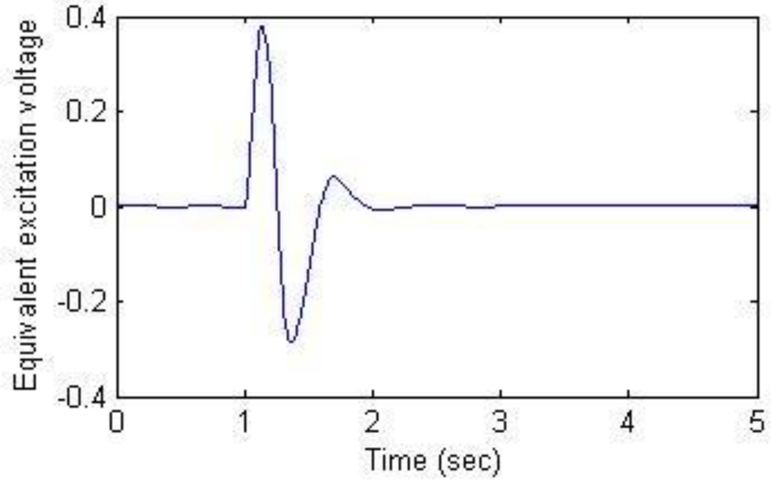

Fig.34: Response of Equivalent Excitation Voltage (ΔE_{fd})

4.5.3 Heavy Loading

As mentioned earlier, in case of heavy loading, per unit values for real and reactive powers are considered to be 1.4 and 0.4, respectively. The TCSC controller signal is shown in Fig.35. It is to be mentioned that the controller signal is common for all the cases, but it is put in every cases may be due to the need of clear and easy comparison of the controller signal with the oscillation problem signals. The responses of the rotor angle ($\boldsymbol{\delta}$), rotor speed ($\boldsymbol{\omega}$), internal voltage behind X_d' ($\boldsymbol{E_q}'$) and equivalent excitation voltage ($\Delta \boldsymbol{E_{fd}}$) are illustrated in Fig.36, 37, 38 and 39, respectively.

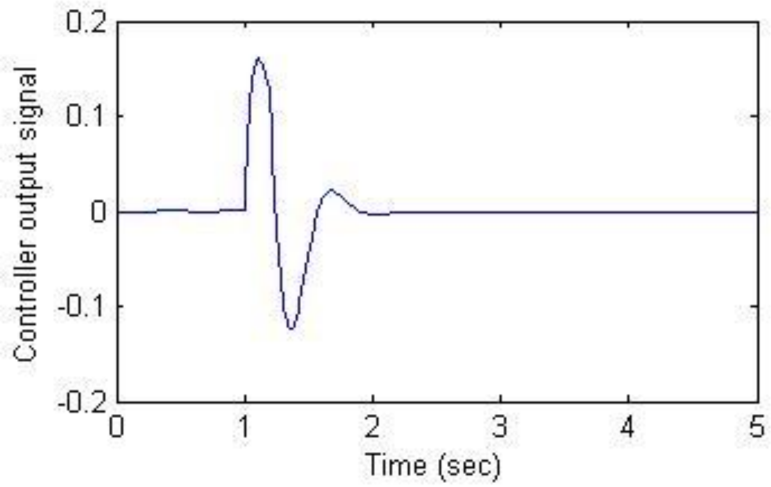

Fig.35**:** Response of the controller output ($\Delta\sigma$)

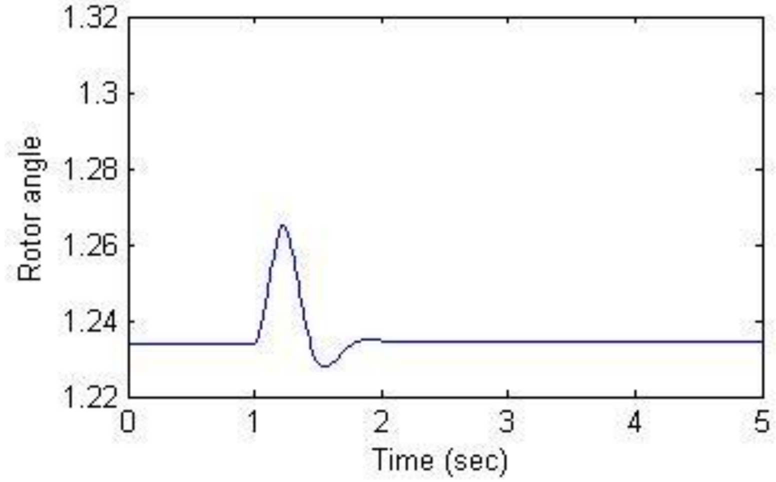

Fig.36**:** Response of Rotor angle (δ)

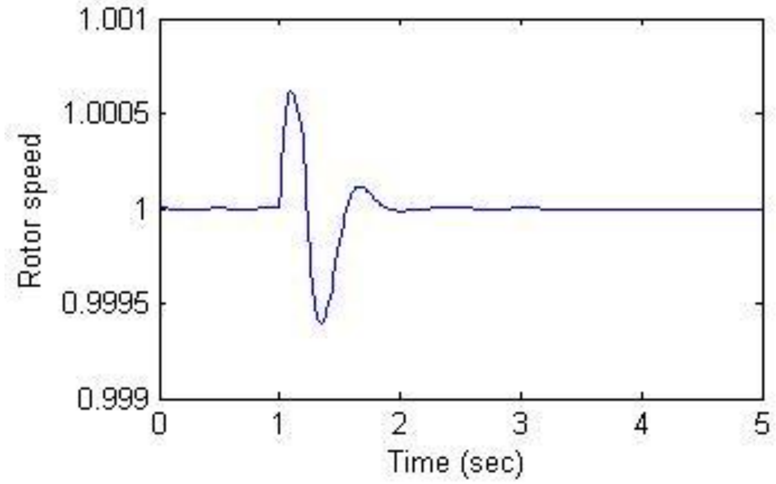

Fig.37**:** Response of Rotor speed (ω)

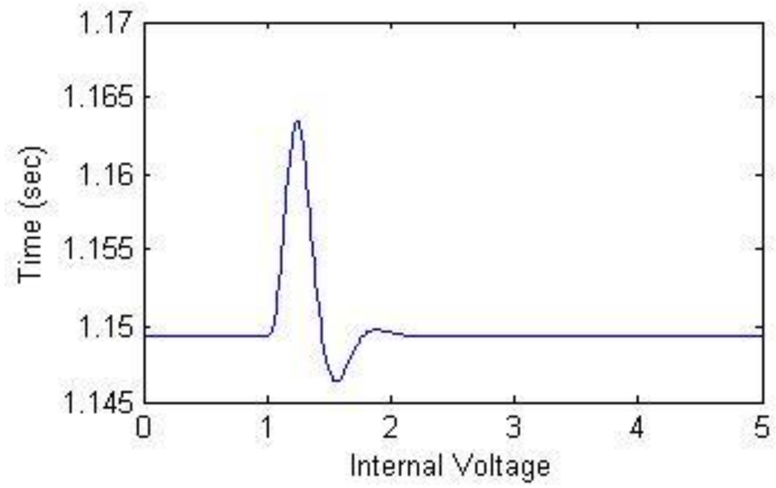

Fig.38**:** Response of Internal voltage behind X_d' ($E_q{}'$)

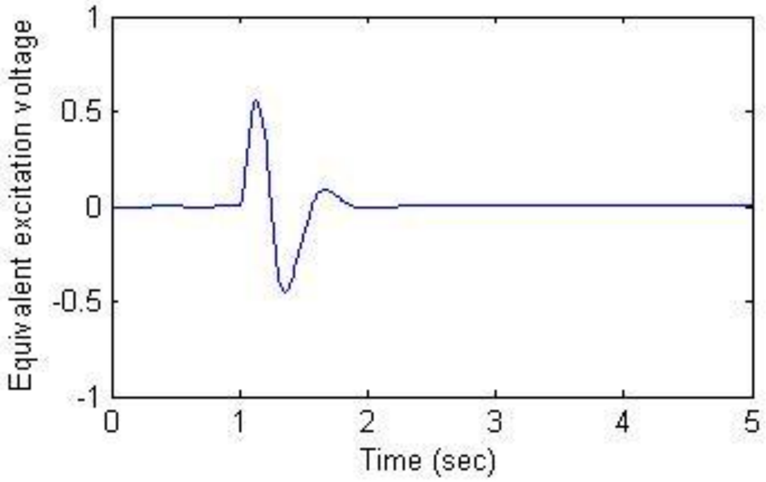

Fig.39**:** Response of Equivalent Excitation Voltage (ΔE_{fd})

Chapter 5

CONCLUSION

This paper presents the power system stability improvement by a TCSC controller. The design of the TCSC controller to improve the power system stability is transformed into a multi objective optimization problem, where IWO optimization algorithm is used to optimize the system parameters. To prove the effectiveness of the TCSC controller in different loading conditions, the TCSC controller is tested with three loading conditions: light loading, nominal loading and heavy loading.

The cost function convergences of the parameters are shown in Fig.10, Fig.11 and Fig.12 for each loading. The algorithm finds the fit parameters in a very short time, showing the effectiveness of IWO over other optimization algorithms proposed by other designs. To show the fast convergence of the algorithm over other approaches proposed by other authors, a comparison of IWO versus a Multi-objective Genetic Algorithm, proposed by [2], is shown in Fig.40 and Fig.41.

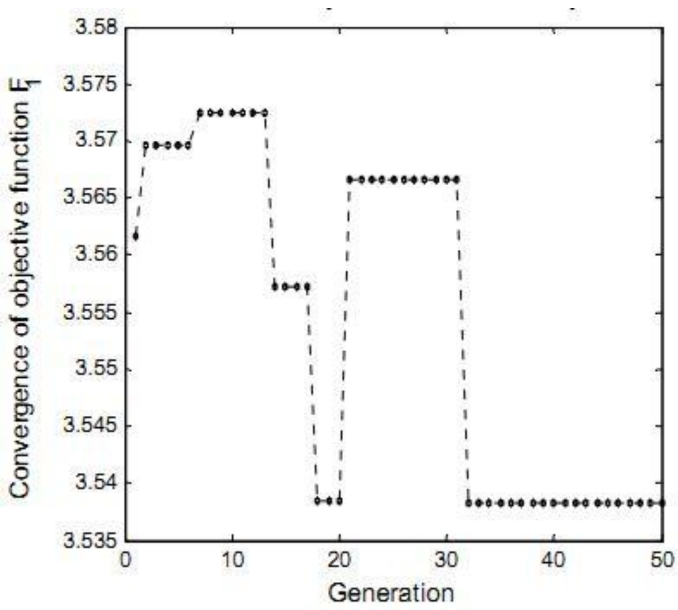

Fig.40: Cost function convergence with Multi-objective Genetic Algorithm

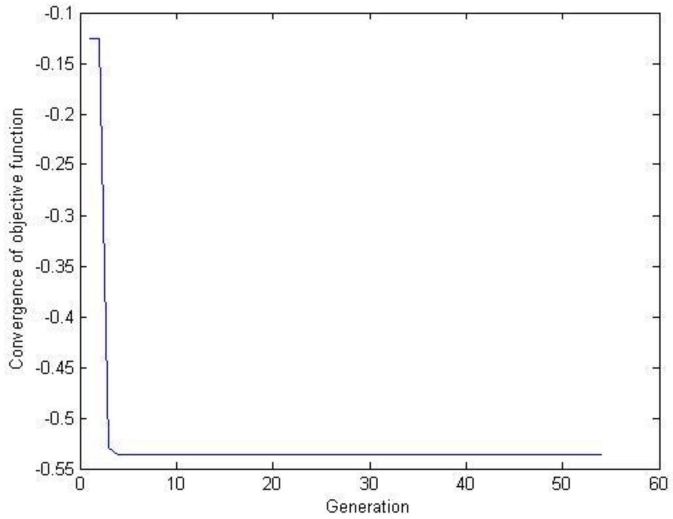

Fig.41: Cost function convergence with IWO Algorithm

Comparing Fig.40 with Fig.41, it observes that how much IWO algorithm is effective than the Multi-objective Algorithm.

The optimized parameters are shown in Table 2 and the System eigenvalues without TCSC controller for three conditions are shown in Table 3, where, the system damping ratios and eigenvalues with TCSC controller for three conditions is shown in Table 4. The more the system values are far from the coordinate system, to that extends the system is stable, whereas; Table 4 shows how much our values are far from the system and is more stable. To show the stability suitable values then Genetic algorithm, the eigenvalues of [2] is quoted below:

Table 5: Eigenvalues of [2]

Without TCSC	With TCSC Controller		
	Solution-1	Solution-2	Solution-3
0.5491± 6.4386i	-1.9987±9.3375i	-0.7636±2.0511i	-2.2561±3.9195i
10.5996±3.8708i	-11.4768±5.4086i	-9.6266±7.7772i	-7.9520±6.8104i
	-13.6599	-74.4628	-23.4994
	-2.6686	-3.3	-6.2253
	-0.1031	-0.1029	-0.1018

The fast damping performance of the TCSC controller over rotor angle and rotor speed as a sample of many parameters, are shown in the result figures, showing how fast the TCSC acts to damp the oscillations in the system. To show the fast and well damping response of our TCSC controller design over other designs proposed, again the rotor speed damping of our design and design by [2] are shown in Fig.42 and Fig.43, respectively, as an example.

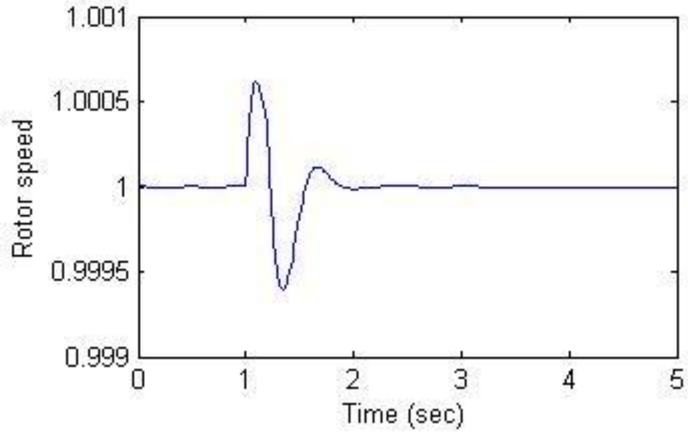

Fig.42: Rotor speed oscillation problem damping by our TCSC controller design

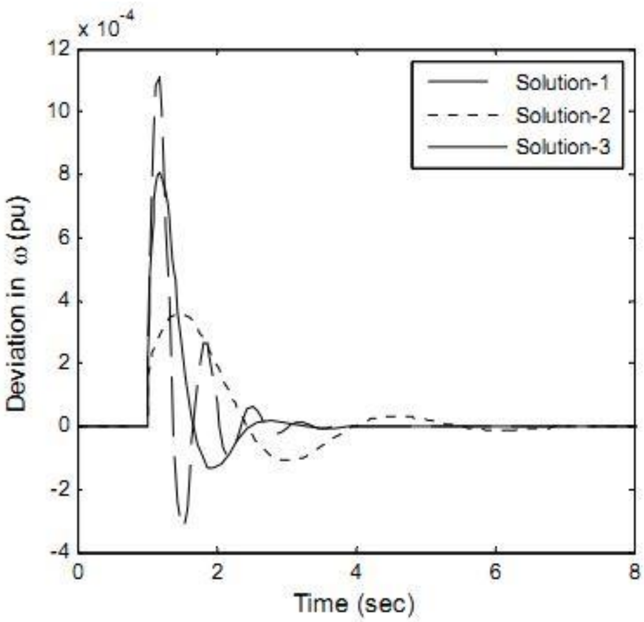

Fig.43: Damping of rotor speed oscillation problem by [2]

Comparing Fig.42 with Fig.43, we observe that how fast and properly our TCSC controller acts to damp the oscillation problems than the design done by [2].

References

[1] K. R. Padiyar, *Power System Dynamics Stability and Control*
[2] Sidhartha Panda, R.N.Patel, N.P.Padhy, *Power System Stability Improvement by TCSC Controller Employing a Multi-Objective Genetic Algorithm Approach*. International Journal of Electrical and Computer Engineering 1:7 2006
[3] P. Kundur, *Power System stability and control.* New York: McGraw-Hill, 1994.
[4] Laiq Khan, IkramUllah, Tariq Saeed, K.L. Lo, *"Virtual Bees Algorithm Based Design of Damping Control System for TCSC",* Australian Journal of Basic and Applied Sciences, 4(1): 1-18, 2010.
[5] B. H Li, Q. H. Wu, D. R. Turner, P. Y. Wang and X.X Zhou, "Modeling of TCSC dynamics for control and analysis of power system stability," *Electrical Power & Energy Systs.*, Vol-22, pp. 43–49. 2000.
[6] A. D Del Rosso, C. A Canizares and V.M. Dona, "A study of TCSC controller design for power system stability improvement, "*IEEE Trans. Power Systs.*, vol-18, pp. 1487-1496. 2003.
[7] Ali Darvish FALEHI, *"Simultaneous Coordinated Design of TCSC-Based Damping Controller and AVR Based on PSO Technique",* Izeh Branch, Islamic Azad University,Iran.
[8] Yao-Nan Yu, *Power System Dynamics*, Academic press Inc., London, 1983.
[9] Sidhartha Panda and N. P. Padhy, "*Thyristor Controlled Series Compensator-based Controller Design Employing Genetic Algorithm:A Comparative Study*". International Journal of Electronics, Circuits and Systems Volume 1 Number 1.
[10] Ashik Ahmed and B. M. Ruhul Amin, *"Optimizaiton of Power System Stabilizer for Multi-Machine Power System using Invasive Weed Optimization Algorithm",* International Journal of Computer Applications(0975-8887) Volume 39-No.7, Feb. 2012.